

Design of Planar Waveguides With Prescribed Mode-Profile Using Inverse Scattering Theory

Itay Hirsh, Moshe Horowitz, and Amir Rosenthal

Abstract—We demonstrate a new method based on inverse scattering theory for designing the refractive index profile of single-mode planar waveguides in order to obtain a desired TE-mode profile. The method enables a direct design of the waveguide profile without the need for iterative optimization algorithms. The design is based on a first order solution to the Gel'fand–Levitan–Marčenko integral equation that gives a simple linear connection between a small change in the scattering data and the corresponding change in the kernel function. This connection reduces the design problem to a simple linear constrained minimization problem which has an explicit solution. Our design method allows adding additional constraints on the refractive index profile such as the waveguide width. The method presented in this paper can be expanded to analyze TM modes and for designing multi-mode planar waveguides.

Index Terms—Inverse problems, optical planar waveguides.

I. INTRODUCTION

THE properties of optical waveguide structures such as the mode profile or dispersion are very important for the design of optical components and optical systems. Although various waveguide structures have been studied thoroughly over the years, the design of waveguides is still a challenging task that has not been solved yet. Previous work on waveguide design were based on specific designs or on various iterative optimization methods [1]–[3].

Even in the simplest cases that of analyzing the TE mode in planar waveguides without a loss, an implicit connection between the waveguide properties and the refractive index of an arbitrary waveguide profile has not been obtained. In a lossless planar waveguide, the inverse problem gives a relation between the reflection coefficients of the waveguide and the propagation constants of the guided modes to the refractive index profile of the waveguide. This relation, given by the Gel'fand–Levitan–Marčenko (GLM) integral equation, is obtained by applying the inverse scattering transform (IST) to a Schrödinger-like equation written for the TE-modes electric field in a planar waveguide. However, since the reflection coefficients are not directly connected to the desired properties of the waveguide, the design still remains a challenging task. Waveguides can be designed based on analytical solutions of

the GLM equation for a reflectionless solution [4]. For such specific waveguides the GLM equation has been used for the design of waveguide profile parameters that support several guided modes with prescribed propagation constants.

A rational reflection coefficient with three poles also gives an analytical solution of the GLM equation [5]–[7]. This approach ensures the design of a single mode waveguide. By changing the poles parameters, different waveguide profiles can be designed. However, there is no direct connection between the waveguide properties and the poles.

Numerical methods for solving the GLM equation have been published [8], [9] under the assumption that the reflection coefficients and the propagation constants of the modes are known. However, in a design problem the reflection coefficients of the waveguide are not known and are not directly connected to the desired waveguide properties.

In our work, we demonstrate a new method for designing the mode profile of a TE-mode in single-mode planar waveguides. The method is based on a linearization of the GLM equation for a planar single-mode waveguide around a known solution. The solution of the linearization gives a linear connection between the scattering data of the waveguide, the refractive index profile, and the mode profile. This solution transforms the design process into a simple linear constrained minimization problem. The solution also easily allows the imposition of additional constraints on the refractive index profile such as the waveguide width, the maximum refractive index value, etc. The solution gives a waveguide with a mode profile that is very similar to the desired mode profile. The difference between the desired profile and the mode profile that is obtained from the design is due the linearization of the GLM equation. Moreover, nonphysical desired profiles induce error and we do not know *a priori* whether or not the desired mode profile is consistent. Nevertheless, our design approach gives a new design tool that enables, for the first time to our knowledge, without using complicated iterative algorithms, the design of planar waveguides with a prescribed TE-mode profile.

II. THEORETICAL BACKGROUND

In this section we describe the main mathematical background that is required to our design of TE-modes in planar waveguides.

A. Planar Waveguides

The propagation of light in an inhomogeneous linear lossless dielectric media can be described, in the frequency domain, assuming an electric field $\tilde{\mathbf{E}}(\mathbf{r}, t) = \mathbf{E}(\mathbf{r})e^{-i\omega t}$, as [10]

$$\nabla^2 \mathbf{E} + \nabla \left[\frac{1}{\epsilon(\omega)} \nabla \epsilon(\omega) \cdot \mathbf{E} \right] + \frac{\omega^2}{c^2} \epsilon(\omega) \mathbf{E} = 0 \quad (1)$$

Manuscript received October 24, 2008; revised January 30, 2009. Current version published August 26, 2009.

I. Hirsh and M. Horowitz are with the Department of Electrical Engineering, Technion - Israel Institute of Technology, Haifa 32000, Israel.

A. Rosenthal is with the Institute for Biological and Medical Imaging (IBMI), Technische Universität and Helmholtz Zentrum München, Neuherberg, Munich 85764, Germany.

Color versions of one or more of the figures in this paper are available online at <http://ieeexplore.ieee.org>.

Digital Object Identifier 10.1109/JQE.2009.2020568

where ϵ is the relative permittivity. In a planar waveguide where the refractive index varies only in a single direction, x , the electric field of the TE modes equals [10]

$$\mathbf{E} = \phi(x)e^{i\beta z}\hat{y} \quad (2)$$

where \hat{y} is the unit vector in the y direction, $\phi(x)$ is the electric field profile, and β is the propagation constant. Substituting (2) into (1) yields a scalar wave equation for the electric field amplitude [10]:

$$\frac{d^2\phi(x)}{dx^2} + \left[\frac{\omega^2}{c^2} n^2(x) - \beta^2 \right] \phi(x) = 0 \quad (3)$$

with $n(x)$, the refractive index profile, defined as $n(x) = \sqrt{\epsilon(x)}$.

In order to be able to use methods developed in the field of Inverse Scattering Theory (IST) on (3) we require that the potential (i.e., $\omega^2/c^2 n^2(x)$) has to decay to 0 at $x \rightarrow \pm\infty$. Clearly, this is not the case since $n(x) \geq 1$. We limit our analysis to profiles with the same asymptotic refractive index values at $x \rightarrow \pm\infty$ [4]:

$$\begin{aligned} \lim_{|x| \rightarrow \infty} n(x) &= n_\infty \\ q(x) &= \frac{\omega^2}{c^2} n^2(x) - \frac{\omega^2}{c^2} n_\infty^2 \\ k^2 &= \frac{\omega^2}{c^2} n_\infty^2 - \beta^2. \end{aligned} \quad (4)$$

Substituting (4) into (3), we have [4]

$$\frac{d^2\phi(x)}{dx^2} + [q(x) + k^2] \phi(x) = 0. \quad (5)$$

Equation (5) can be also used to analyze TM modes, with $\phi(x)$ and $q(x)$ defined as [7]

$$\begin{aligned} \phi(x) &= \epsilon(x)^{(1/2)} E_x, \\ q(x) &= \frac{\epsilon''(x)}{2\epsilon(x)} - \frac{3}{4} \left[\frac{\epsilon'(x)}{\epsilon(x)} \right]^2 + \frac{\omega^2}{c^2} [\epsilon(x) - n_\infty^2] \end{aligned} \quad (6)$$

where E_x is the x component of the electric field and the tag $'$ sign represents a derivative with respect to x .

B. Inverse Scattering Theory in Planar Waveguides

Equation (5) is the scalar Schrödinger eigenvalue problem with a decaying potential. Therefore, it can be solved by using IST. The use of IST to study the scalar Schrödinger equation is described in detail in [11]. We will give below the main results needed for our design method. The analysis can be expanded to analyze TM modes in planar waveguides [4].

In order to define the scattering data, three solutions of the Schrödinger equation are chosen: $\phi(k, x)$, $\psi(k, x)$, $\bar{\psi}(k, x)$ with the following boundary conditions [11]:

$$\begin{aligned} \phi(k, x) &\sim e^{-ikx}, \quad x \rightarrow -\infty \\ \psi(k, x) &\sim e^{ikx}, \quad \bar{\psi}(k, x) \sim e^{-ikx}, \quad x \rightarrow \infty. \end{aligned} \quad (7)$$

Since the two solutions $\psi(k, x)$, $\bar{\psi}(k, x)$ are independent [11], the solution $\phi(k, x)$ can be expressed as a linear combination of the two solutions:

$$\phi(k, x) = a(k)\bar{\psi}(k, x) + b(k)\psi(k, x). \quad (8)$$

The reflection coefficient $r(k)$ and the transmission coefficients $t(k)$ are defined using the functions $a(k)$, $b(k)$ as follows [11]:

$$\begin{aligned} r(k) &= \frac{b(k)}{a(k)} \\ t(k) &= \frac{1}{a(k)}. \end{aligned} \quad (9)$$

The two independent functions $\bar{\psi}(k, x)$, $\psi(k, x)$ can be represented as [11]

$$\begin{aligned} \psi(k, x) &= e^{ikx} + \int_x^\infty K(x, s)e^{iks} ds \\ \bar{\psi}(k, x) &= e^{-ikx} + \int_x^\infty K(x, s)e^{-iks} ds \end{aligned} \quad (10)$$

where $K(x, y)$ is a kernel function that is identical for both solutions. Equations (5) and (10) result in the GLM integral equation for $K(x, y)$ [11]:

$$K(x, y) + F(x+y) + \int_x^\infty K(x, s)F(s+y)ds = 0 \quad (11)$$

where

$$\begin{aligned} F(x) &= \sum_j C_j e^{-\kappa_j x} + h(x) \\ h(x) &= \mathcal{F}_x[r(k)] \equiv \frac{1}{2\pi} \int_{-\infty}^\infty r(k)e^{ikx} dk. \end{aligned} \quad (12)$$

In input data for the GLM equation are the mode coefficients κ_j and C_j and the impulse response $h(x)$. The potential, $q(x)$, can be derived from the kernel function by [11]

$$q(x) = 2 \frac{d}{dx} K(x, x). \quad (13)$$

For the j th guided mode the reflection coefficient $r(k)$ has a pole on the positive imaginary axis at a point $k = i\kappa_j$ with residue iC_j . The field of the j th mode, $\phi_j(x)$, is given using (8)–(10), by

$$\phi_j(x) = \frac{r(i\kappa_j)}{t(i\kappa_j)} \left[e^{-\kappa_j x} + \int_x^\infty K(x, s)e^{-\kappa_j s} ds \right] \quad (14)$$

where $K(x, y)$ is the solution of (11). The poles κ_j are connected to the guided modes propagation constants β_j as shown in (4). The poles also give the decay of the guided modes at $x = \pm\infty$ [11]:

$$\begin{aligned} \phi_j(x) &\rightarrow \frac{r(i\kappa_j)}{t(i\kappa_j)} e^{-\kappa_j x}, \quad x \rightarrow \infty \\ \phi_j(x) &\rightarrow e^{\kappa_j x}, \quad x \rightarrow -\infty. \end{aligned} \quad (15)$$

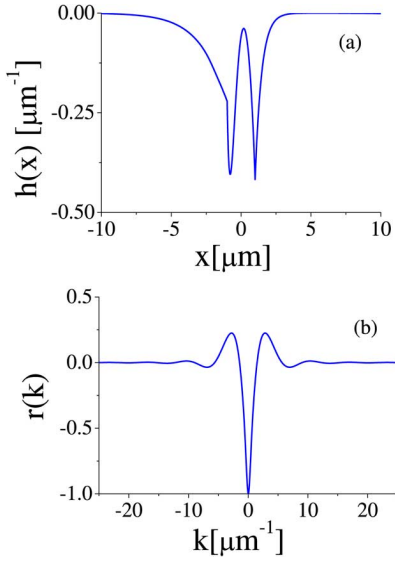


Fig. 1. (a) Impulse response $h(x)$ and (b) reflection coefficient $r(k)$ of a single mode 3-layer slab waveguide with a width of $1 \mu\text{m}$ at a wavelength of $1.5 \mu\text{m}$.

The total power of the j th guided mode is given [11]:

$$\int_{-\infty}^{\infty} [\phi_j(x)]^2 dx = \left[\frac{r(i\kappa_j)}{t(i\kappa_j)} \right]^2 \frac{1}{C_j}. \quad (16)$$

The reflection coefficient function $r(k)$ that is defined on the real axis k or its Fourier transform, the impulse response $h(x)$, represent the radiative and the evanescent modes [12]. The impulse response should be a continuous function with possible discontinuities in its derivative. When assuming a semi-finite potential with nonzero values at the region $(-\infty, L]$ the impulse response obeys

$$h(x > 2L) = - \sum_j C_j e^{-\kappa_j x} \quad (17)$$

due to the causality of $F(x)$, $F(x > 2L) = 0$ [5]. Fig. 1 shows the reflection coefficient and impulse response of a single mode slab waveguide with a core in the region $[-0.5, 0.5] \mu\text{m}$. The refractive index of the core and the cladding are equal to $n_{co} = 1.2$ and $n_{cl} = 1$ respectively. The results are calculated at a wavelength $\lambda = 1.5 \mu\text{m}$ using transfer matrix method [13]. The figure shows the discontinuities of the impulse response derivative at the waveguide ends at $x = \pm 2L$ as well as the exponential behavior of the function at $x > 2L$ as described by (17).

III. APPROXIMATE SOLUTION TO THE GLM EQUATION

The inverse scattering method gives a connection between the scattering data and the waveguide mode profile. However, the connection between the scattering data and the mode profile is highly nonlinear. Therefore, the solution of the problem requires optimization methods with a long computation duration. We have developed a simple approximation to the solution of the GLM equation that gives an explicit linear connection between a perturbation in the reflection coefficient $r(k)$ and the

corresponding perturbation in the solution to the GLM equation, $K(x, y)$. This approximation is based on a first order expansion of the GLM equation around a known zero order solution. We will use a zero order solution that corresponds to a reflectionless waveguide that supports only a single mode with a known propagation constant.

We assume that the kernel function $K_0(x, y)$ is a solution of the GLM equation for the scattering data $F_0(x)$. Adding a small perturbation to the scattering data $F(x) = F_0(x) + \varepsilon F_1(x)$ results in a small change in the kernel function $K(x, y) = K_0(x, y) + \varepsilon K_1(x, y)$. The GLM equation for the functions $K(x, y)$, $F(x)$ is given by

$$\begin{aligned} 0 = & K_0(x, y) + F_0(x + y) + \int_x^\infty K_0(x, s) F_0(s + y) ds \\ & + \varepsilon K_1(x, y) + \varepsilon F_1(x + y) \\ & + \varepsilon \int_x^\infty K_1(x, s) F_0(s + y) ds \\ & + \varepsilon \int_x^\infty K_0(x, s) F_1(s + y) ds \\ & + \varepsilon^2 \int_x^\infty K_1(x, s) F_1(s + y) ds. \end{aligned} \quad (18)$$

The first three terms in the right-hand side of (18) are equal to zero. By assuming that $F_1(x)$ is of the same order of magnitude as $F_0(x)$ and requiring that $\varepsilon \ll 1$, we can neglect terms of the order of ε^2 and obtain

$$\begin{aligned} K_1(x, y) + F_1(x + y) + \int_x^\infty K_1(x, s) F_0(s + y) ds \\ + \int_x^\infty K_0(x, s) F_1(s + y) ds = 0. \end{aligned} \quad (19)$$

We perform the linearization of the GLM equation around a zero-order solution $K_0(x, y)$ that corresponds to a reflectionless potential, $r(k) = 0$, of a single mode waveguide. We also assume that the propagation constant β is given. For a single mode reflectionless waveguide, the zero-order scattering data equals

$$F_0(x) = C e^{-\kappa x}. \quad (20)$$

This scattering function gives an explicit expression for $K_0(x, y)$ [4]:

$$K_0(x, y) = - \frac{2\kappa C e^{-\kappa x}}{2\kappa + C e^{-2\kappa x}} e^{-\kappa y}. \quad (21)$$

By assuming that the perturbation only changes the impulse response and not the mode coefficients C and κ we obtain

$$F_1(x) = h(x) \quad (22)$$

where $h(x)$ is the impulse response after the perturbation. The solution of (19) is derived in the Appendix. The result gives an approximate solution to the GLM equation, $K(x, y) = K_0(x, y) + K_1(x, y)$:

$$\begin{aligned} K(x, y) = & K_0(x, y) - \mathcal{F}_{x+y} [r(k)] - K_0(x, x) \mathcal{F}_{x+y} \left[\frac{r(k)}{\kappa - ik} \right] \\ & - K_0(x, y) \left(K_0(x, x) \mathcal{F}_{2x} \left[\frac{r(k)}{(\kappa - ik)^2} \right] + \mathcal{F}_{2x} \left[\frac{r(k)}{\kappa - ik} \right] \right) \end{aligned} \quad (23)$$

where \mathcal{F}_x is the inverse Fourier transform operator defined in (12). We can also express $K(x, y)$ in terms of the impulse response:

$$\begin{aligned} K(x, y) &= -K_0(x, x)e^{\kappa(x+y)} \int_{x+y}^{\infty} h(s)e^{-\kappa s} ds \\ &\quad - K_0(x, y)e^{2\kappa x} \left(K_0(x, x) \int_{2x}^{\infty} h(s)(s-2x)e^{-\kappa s} ds \right. \\ &\quad \quad \left. + \int_{2x}^{\infty} h(s)e^{-\kappa s} ds \right) \\ &\quad - h(x+y) + K_0(x, y). \end{aligned} \quad (24)$$

The refractive index profile can now be calculated by using (4) and (13).

By substituting (24) into (14), we obtain an explicit expression that connects the guided mode profile and the impulse response:

$$\begin{aligned} \phi(x) = e^{-\kappa x} \left[1 + \frac{K_0(x, x)}{2\kappa} \right] &\left(1 - e^{2\kappa x} \int_{2x}^{\infty} h(s)e^{-\kappa s} ds \right. \\ &\quad \left. - K_0(x, x)e^{2\kappa x} \int_{2x}^{\infty} h(s)(s-2x)e^{-\kappa s} ds \right). \end{aligned} \quad (25)$$

This linear connection will be used in the next section to design the waveguide.

The quality of the reconstruction depends on the magnitude of the perturbation in the function $F(x)$.

In order to demonstrate the accuracy of the linearization, we numerically analyzed two refractive index profiles that were obtained by changing the refractive index profile of an hyperbolic secant waveguide that corresponds to a reflectionless waveguide. The impulse response and the mode coefficients C and κ were calculated separately for each of the refractive index profiles using the transfer matrix method [13]. Then, by using (13) and (24) we have calculated the refractive index profile and compared the result to the original refractive index profile. For each waveguide, the linearization of the GLM solution was performed about a reflectionless waveguide with the parameters C and κ that was calculated for that profile. Fig. 2 shows the reconstructed and the original refractive index profiles. The figures shows that the linearization caused a very small error in the reconstruction.

IV. OPTIMIZATION PROCEDURE

The problem we intend to solve in this manuscript is to design a single-mode planar waveguide with a prescribed TE-mode profile. The width of the nonuniform region of the waveguide equals $2L_w$ and the mode profile equals

$$\phi_d(x) = \left\{ \begin{array}{ll} e^{\kappa x} & x < -L_w \\ \phi_m(x) & -L_w \leq x \leq L_w \\ \phi_m(L_w)e^{-\kappa(x-L_w)} & x > L_w \end{array} \right\}. \quad (26)$$

In order to design the waveguide one should prescribe the mode profile in the region where the refractive index can be controlled, $\phi_m(x)$ and also prescribe the mode coefficient κ that determines the attenuation of the mode in the cladding. The

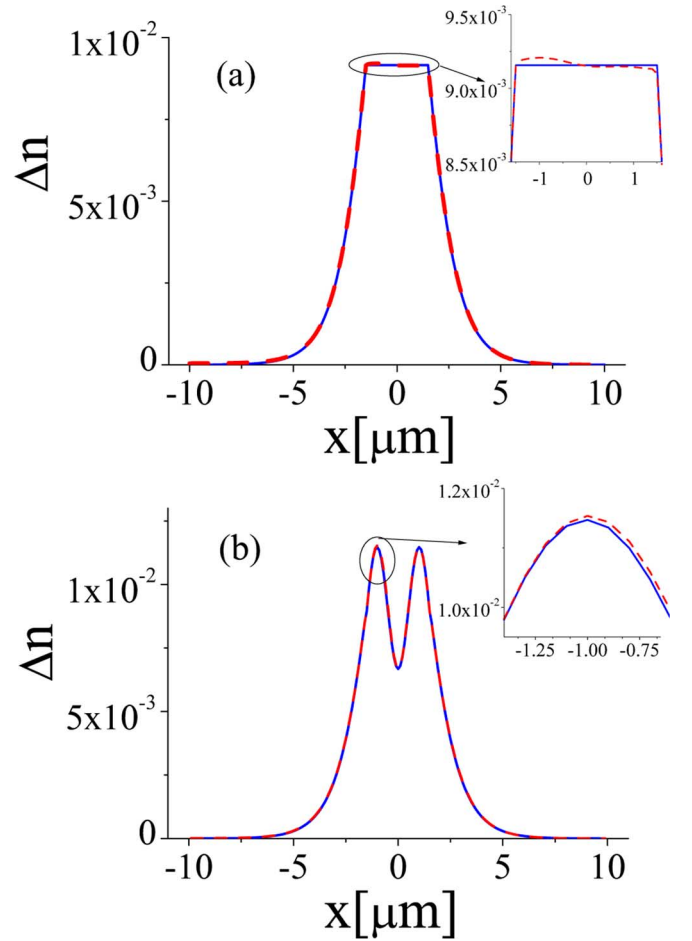


Fig. 2. Comparison between the original and the extracted refractive index profiles that were reconstructed from the linearized GLM equation. Both profiles were obtained by changing the refractive index profile of an hyperbolic secant waveguide that corresponds to a reflectionless waveguide. An excellent agreement between the reconstructed (dotted line) and the original (solid line) profiles was obtained for (a) a truncated hyperbolic secant profile and (b) a sinusoidal perturbation.

mode profile should be a continuous function with a continuous derivative. We note that the definition of the mode profile in (26) does not assume that the total mode power is equal to 1 as is often assumed in waveguide analysis.

In order to calculate the refractive index profile of a single mode waveguide with a prescribed mode profile we solve an optimization problem. We require the mode profile of the waveguide, ϕ to be as close as possible to the desired mode field ϕ_d . Mathematically, we look for a waveguide mode that minimizes the square error between the waveguide mode and the desired mode profiles. We choose to solve a minimization problem rather than give an accurate solution to the problem since the desired profile may not be always attainable in a waveguide with a finite width and a finite refractive index. Moreover, the problem is ill conditioned by its nature. Waveguides with different structures may give a similar mode profile. There might be also a difference between the mode profiles of substantially different waveguides in regions where the mode amplitude is weak. Optimization procedures also enable the imposition of constraints on the solution such as practical limitations on the waveguide width or on the maximum refractive index change.

We start the design by calculating the parameter C using (15) and (16):

$$C = \left[\frac{\phi_d(x)}{\phi_d(-x)} \right]^2 \frac{1}{\int_{-\infty}^{\infty} \phi_d(x')^2 dx'} \quad x > L_w. \quad (27)$$

The connection between the mode field $\phi(x)$ and the impulse response is given by the linearized equation-(25). The impulse response can then be obtained by solving the following Lagrange constrained optimization problem:

$$\begin{aligned} h(x) &= \arg \min_{h(x)} \|\phi_d(x) - \phi(x)\|^2 \\ \text{subject to} \quad & 1. \int_{-\infty}^{\infty} h(x) dx = -1. \\ & 2. \text{Im}[h(x)] = 0 \end{aligned} \quad (28)$$

where $\|f(x)\|^2 = \int_{-\infty}^{\infty} |f(x)|^2 dx$. The first constraint is obtained in a finite waveguide since $r(k=0) = -1$ [14] and the second constraint is obtained since the waveguide is lossless [15]. Other constraints on the impulse response may be added depending on limitations that can be imposed on the waveguide structure such as the maximum allowable change in refractive index or the maximum waveguide width $2L_w$.

We implement the minimization problem described by (28) by discretizing the problem along the x -axis. We assume that the waveguide is uniformly sampled in the analyzed region $[-L, L]$ with a step size Δ , where L is chosen to be significantly larger than the width of the mode field L_w . The integrals in (25) are then replaced by Riemann sums. The discrete form of (25) is given by

$$\bar{\phi} = \bar{\theta} \bar{h} + \bar{\varphi} \quad (29)$$

where bar and double bar represent a vector and a matrix, respectively, $x_i = -L + i\Delta$, $\phi_i = \phi(x_i)$,

$$\begin{aligned} h_i &= h(2x_i), \quad \varphi_i = e^{-\kappa x_i} \left(1 + \frac{K_0(x_i, x_i)}{2\kappa} \right), \\ \theta_{ij} \quad |_{j < i} &= 0, \\ \theta_{ij} \quad |_{j \geq i} &= -2\Delta(1 + 2x_j - 2x_i) e^{\kappa(x_i - 2x_j)} \left(1 + \frac{K_0(x_i, x_i)}{2\kappa} \right) \end{aligned} \quad (30)$$

and $i, j = 1, 2, 3, \dots, N = 2L/\Delta + 1$.

Substituting (29) into the minimization problem presented in (28) results in the linear quadratic system with constraints:

$$\begin{aligned} \text{minimize} \quad & \frac{1}{2} \bar{h}^T \bar{Q} \bar{h} + \bar{c}^T \bar{h} \\ \text{subject to} \quad & \bar{A}^T \bar{h} = b \end{aligned} \quad (31)$$

where

$$\begin{aligned} \bar{Q} &= \bar{\theta}^T \bar{\theta}, \quad \bar{c} = \bar{\theta}^T (\bar{\varphi} - \bar{\phi}_d), \\ A_i &= \Delta, \quad b = -\frac{1}{2}. \end{aligned} \quad (32)$$

The first constraint given in (28) is implemented by approximating the integral as a Riemann sum using the vector \bar{A} and the scalar b . The second constraint that $h(x)$ should be real is a direct result of (33).

In case that \bar{Q} is a positive definite matrix, the solution of the quadratic system given in (31) equals to [16]

$$\bar{h} = \bar{Q}^{-1} \bar{A} (\bar{A}^T \bar{Q}^{-1} \bar{A})^{-1} [\bar{A}^T \bar{Q}^{-1} \bar{c} + b] - \bar{Q}^{-1} \bar{c}. \quad (33)$$

Since the matrix \bar{Q} is not necessarily positive definite and since in most examples that we checked the matrix \bar{Q} was ill-conditioned we could not use directly (33). Equation (25) indicates that $\phi(x)$ has a weak dependence on the values of the impulse response for $|x| \gg \kappa^{-1}$. Therefore, different impulse response functions will result in similar mode profiles and hence in most examples we analyzed the matrix \bar{Q} has a large condition number.

In order to overcome the ill-conditioned problem we use the Tikhonov regularization method [17]. This method stabilizes the solution and ensures the possibility to numerically invert the matrix \bar{Q} . The Tikhonov regularization method also ensures that the matrix \bar{Q} will become positive definite as required for the solution given in (33).

The Tikhonov regularization method is obtained by adding a positive real constant α to the diagonal of \bar{Q} :

$$\bar{Q}_{\text{new}} = \bar{Q} + \alpha \bar{I} \quad (34)$$

where \bar{I} is the unit matrix. Then, the solution to the system is obtained by replacing \bar{Q} with \bar{Q}_{new} in (33). The eigenvalues of the matrix \bar{Q}_{new} are shifted by α compared to the that of the matrix \bar{Q} . Therefore, in order to ensure that \bar{Q} is positive definite α must be larger than the absolute value of the most negative eigenvalue of \bar{Q} . However, when the value of α is too high the error in the mode profile becomes large. Our numerical results shows that reasonable values for α are in the range of 1%–30% of the largest positive eigenvalue of \bar{Q} . This choice ensures that the condition number of the matrix \bar{Q} will be sufficiently low to yield a stable solution. The optimal value for the constant α can be determined by slightly changing the value of α and comparing the mode field that is obtained to the desired mode field. The use of Tikhonov regularization also decreases the absolute value of peaks in the impulse response and hence it improves the accuracy of our linearized solution to the GLM equation. An example of the dependence of the solution accuracy on the choice of the constant α is shown in Section V.

In order to obtain the refractive index we need to solve the GLM equation given in (11) with the scattering data, $F(x) = C e^{-\kappa x} + h(x)$, where C is extracted by using (27), and $h(x)$ is the impulse response obtained using the optimization procedure. Since in the design process we used a linearized solution of the GLM equation we will also use this approximation to solve the GLM equation. The discrete form of (24) after substituting $y = x$ is given by

$$\begin{aligned} K_i &= K(x_i, x_i) = K_0(x_i, x_i) \\ &\times \left(1 - 4\Delta e^{2\kappa x_i} \sum_{j=i}^N h_j e^{-2\kappa x_j} \right. \\ &\quad \left. - 4\Delta K_0(x_i, x_i) e^{2\kappa x_i} \sum_{j=i}^N h_j (x_j - x_i) e^{-2\kappa x_j} \right) - h_i. \end{aligned} \quad (35)$$

The calculation of the potential is then performed by using (13):

$$q(x_i) = 2 \frac{K_{i+1} - K_i}{\Delta}. \quad (36)$$

Equation (35) shows that the errors in the reconstruction increase when x_i decreases. For improving the design accuracy we apply the procedure described from both sides of the waveguide and extract each half side of the waveguide from its corresponding impulse response. Thus, two optimization procedures are performed. In the first optimization we extract half of the waveguide as described above. In the second step we extract the other half of the waveguide by repeating the above described method for $\phi(-x)$ instead of $\phi(x)$. We have checked that the error in the reconstruction can be further decreased by solving the GLM equation for the scattering data obtained in the optimization procedure by using methods as in [18], [19], [20] instead of using (35). Moreover, the scattering data $F(x)$ should correspond to a single mode waveguide. However, we have found that errors in (35) or nonphysical requirements on the mode profile may result in a multi-mode waveguide.

V. NUMERICAL RESULTS

We demonstrate our method for designing the mode profile of a single mode planar waveguide with desired super-Gaussian TE-mode profiles.

In the first example we demonstrate the dependence of the design method on the Tikhonov regularization. In this example the numerical discretization is chosen with resolution $\Delta = 0.04 \mu\text{m}$ and a simulation length $40 \mu\text{m}$ ($L = 20 \mu\text{m}$). The wavelength is equal to 1550 nm . The desired mode has a super-Gaussian profile

$$\phi_d(x) = \begin{cases} e^{\kappa x} & x < -L_w \\ Be^{-(1/2)(x/\sigma)^{2j}} & -L_w < x < L_w \\ e^{-\kappa x} & x > L_w \end{cases} \quad (37)$$

where $j = 3$, $\sigma = 5 \mu\text{m}$. The desired waveguide width was equal to $2L_w = 8 \mu\text{m}$, and the parameters κ , B were chosen in order to obtain a continuous function $\phi_d(x)$ and its derivative at $x = \pm L_w$.

Fig. 3 shows the extracted refractive index profile (a) and the desired mode profile (b) for four values of the Tikhonov parameter α : $\alpha = 2.45 \times 10^{-16}$ (red dashed curve), $\alpha = 2.45 \times 10^{-14}$ (purple dotted curve), $\alpha = 4.9 \times 10^{-13}$ (blue dashed-dotted curve) and $\alpha = 9.8 \times 10^{-13}$ (cyan dashed-dot-dot curve). These parameters are equal to 0.01%, 1%, 20%, and 40% of the maximum eigenvalue of the matrix \bar{Q} . The maximum errors in the nonuniform region of the waveguide are 0.8%, 0.4%, 6%, and 8%, respectively. The mode profile was calculated from the extracted refractive-index profile using transfer matrix method [15]. The results indicate that in our example the optimum result is obtained for $\alpha = 2.45 \times 10^{-14}$. A smaller value of $\alpha = 2.45 \times 10^{-16}$ gives a high change in the refractive index while the error in the mode profile slightly increases. This result is obtained since the condition number of the matrix \bar{Q} becomes too high— 10^4 . Since it is practically desirable to reduce the maximum change in the refractive index, the Tikhonov parameter α should not be chosen to be too small. Larger values

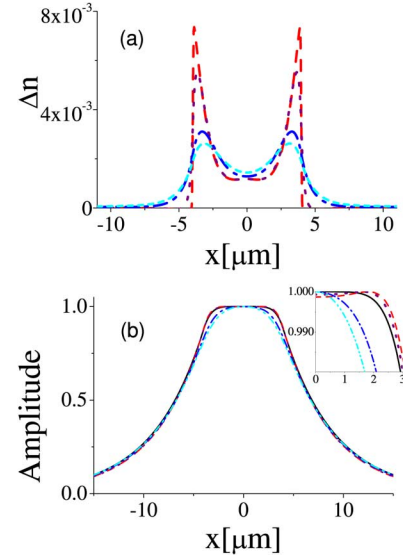


Fig. 3. (a) Designed refractive index profile and (b) the corresponding mode profile of a waveguide with a desired super-Gaussian mode for four different values of the regularization constant α : $\alpha = 2.45 \times 10^{-16}$ (red dashed curve), $\alpha = 2.45 \times 10^{-14}$ (purple dotted curve), $\alpha = 4.9 \times 10^{-13}$ (blue dashed-dotted curve), and $\alpha = 9.8 \times 10^{-13}$ (cyan dashed-dot-dot curve). The desired mode profile is shown as a solid curve. The inset gives a zoom on the mode profile in the middle of the waveguide.

for α give profiles with lower maximum refractive index values. However, in this case, the dependence of the designed profile on the desired mode profile decreases and hence the error in the obtained mode-profile increases as can be seen in Fig. 3(b).

In the next three examples, we demonstrate the capability of our design method to accurately design planar waveguides with different mode profiles. The different mode profiles that were chosen are super-Gaussian as given in (37). The mode coefficients equal to $j = 1, 2, 4$ in Figs. 4–6, respectively. The other parameters are the waveguide width $2L_w = 16 \mu\text{m}$ and $\sigma = 10 \mu\text{m}$. The parameters κ , B were chosen in order to obtain a continuous function $\phi_d(x)$ and derivative at $x = \pm L_w$. The spatial resolution equals $\Delta = 0.16 \mu\text{m}$, the analysis window equals $2L = 160 \mu\text{m}$, and the Tikhonov constant equals in each example to 1% of the largest positive eigenvalue of the matrix \bar{Q} . Due to the small errors in the optimization procedure and in the linearization of the GLM equation the resulting waveguide profile had a width that slightly exceeds $2L_w$. The waveguide width at 10% of the maximum refractive index of the obtained waveguides was about 4%, 6%, and 8% longer than $2L_w$ for $j = 1, 2, 4$, respectively. Therefore, we truncated the waveguide profile at $x = \pm L_w$ in order to get an exact width of the waveguide profile. In all of the waveguides that were designed, the truncation of the waveguide profile did not cause a significant error in the mode-profile as shown below. The runtime of the analysis on a standard personal computer was less than 1 minute.

Figs. 4–6 show the designed refractive index profile and a comparison between the desired super-Gaussian mode profile with parameter $j = 1, 2, 4$ and the obtained mode profile, respectively. The obtained mode profile was calculated from the extracted waveguide profile by using the transfer matrix method [15]. The figure shows a very good quantitative agreement between the desired profiles and the obtained mode profiles. The

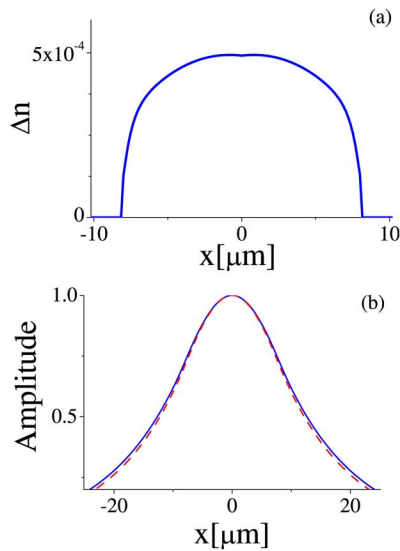


Fig. 4. (a) Designed refractive index profile and (b) corresponding mode profile (red dashed curve) that is compared to the desired mode profile (blue solid curve) for a super-Gaussian waveguide with a width of $16 \mu\text{m}$ and a mode parameter $j = 1$.

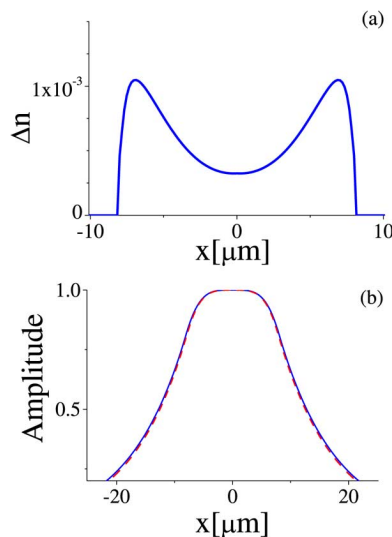


Fig. 5. (a) Designed refractive index profile and (b) corresponding mode profile (red dashed curve) that is compared to the desired mode profile (blue solid curve) for a super-Gaussian waveguide with a width of $16 \mu\text{m}$ and a mode parameter $j = 2$.

maximum relative error between the mode profiles of the desired and the obtained profiles equals 2%, 1.6%, and 1.9% for $j = 1, 2, 4$, respectively. The error in the cladding or the uniform region of the waveguide is calculated as the relative error between the desired and designed mode coefficient κ . The relative error in the mode coefficient κ equals to 4%, 1.9%, 1.3% for $j = 1, 2, 4$, respectively.

We note that our design method is not limited to waveguides with a small change in the refractive index profile as was shown in Figs. 4–6. In the examples that are shown in these figures, the requirements of a single-mode waveguide with the desired waveguide widths and the desired mode profiles resulted

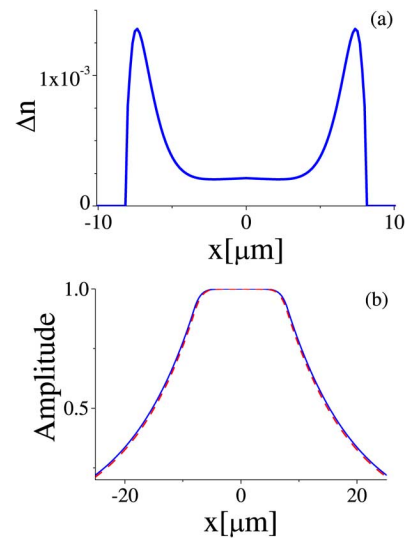


Fig. 6. (a) Designed refractive index profile and (b) corresponding mode profile (red dashed curve) that is compared to the desired mode profile (blue solid curve) for a super-Gaussian waveguide with a width of $16 \mu\text{m}$ and a mode parameter $j = 4$.

in small changes in the refractive index profiles. Our method also enables designing waveguides with a high contrast refractive index profile where the relative change in the refractive index is high. For example, we have successfully designed a single mode waveguide with a width of $2L_w = 2 \mu\text{m}$ and with a super-Gaussian mode profile with parameters $j = 4$ and $\sigma = 1.3 \mu\text{m}$. The design was performed at an optical wavelength of $5 \mu\text{m}$. In this example the obtained peak to peak refractive index difference in the waveguide profile was larger than 0.65. A very good agreement between the desired and the obtained mode profiles was obtained. The maximum relative error between the mode profile of the desired and the obtained profile equals 0.6% and the relative error in the mode coefficient κ equals to 7%. Our design method gives a large error when the linearization used in (19) becomes not valid. Such a case is more likely to occur when the refractive index profile is complicated and the changes in refractive index are high. The error may be avoided by linearizing the solution to the GLM equation around a different waveguide profile than the reflectionless waveguide used in this work.

In the last example, shown in Fig. 5 we show that an increase in the desired waveguide width L_w may result in a multi-mode waveguide. In a waveguide with a super-Gaussian profile, given in (37), an increase in the size of the nonuniform part of the waveguide, L_w , results in an increase in the mode coefficient κ that is required of a continuous mode profile with a continuous derivative. Therefore, the conditions for the emergence of another mode are relaxed. Fig. 7 shows the refractive index profile and the two guided mode profiles for a designed waveguide with $L_w = 10 \mu\text{m}$. The other parameters are the same as in Fig. 5. Fig. 7 shows excellent agreement between the desired mode profile (blue solid curve) and the first guided mode (red dashed curve) with a maximum error of 2.4%. However, in this example small errors in the refractive index profile design cause

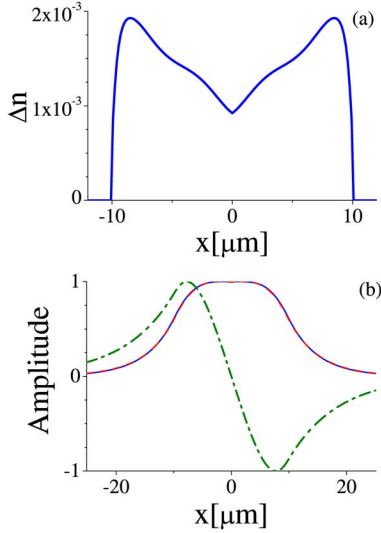


Fig. 7. (a) Designed refractive index profile and (b) obtained mode profile (dashed curve) that is compared to the desired mode profile (solid curve) for a waveguide with a super-Gaussian profile having a width of 20 μm . The other parameters are the same as in Fig. 5.

the generation of a second guided mode that is shown in the green dotted curve in Fig. 7.

VI. CONCLUSION

We have demonstrated a new method, based on inverse scattering theory, for designing the refractive index profile of single mode planar waveguides in order to obtain a desired TE-mode profile. The method enables, for the first time, a direct design of planar waveguides without the need for time-consuming iterative optimization algorithms. The design is based on a first order solution of the GLM equation for a single mode planar-waveguide. By using this approximation we obtain a simple linear relation between a small change in the scattering data of the waveguide and the change in the kernel function. This relation allows us to reduce the design problem to a simple linear constrained minimization problem with an explicit solution. Therefore, our design method does not require time consuming trial and error optimization methods. Our design method also allows the direct imposition of additional constraints on the scattering data or on the refractive index profile such as the waveguide width or the maximum change in the refractive index profile. The method presented in this paper can be also directly implemented for designing multi mode planar waveguides. The method can be also easily extended to analyze TM-modes in waveguides with a relative small change in the refractive index by solving additional differential equation that relates the potential $q(x)$ that is obtained in the design and the refractive index profile [7].

APPENDIX

In this Appendix, we derive a solution to GLM equation based on a linearization about a reflectionless potential of a single-mode planar waveguide. For given mode parameters C and κ , the kernel function $K_0(x, y)$ is calculated by solving the equation

$$K_0(x, y) + Ce^{-\kappa(x+y)} + \int_x^\infty K_0(x, s)Ce^{-\kappa(s+y)} ds = 0. \quad (38)$$

The solution is given by

$$K_0(x, y) = -\frac{2\kappa Ce^{-\kappa(x+y)}}{2\kappa + Ce^{-2\kappa x}}. \quad (39)$$

We proceed by calculating the first-order kernel function $K_1(x, y)$, by solving (19):

$$\begin{aligned} K_1(x, y) + \frac{1}{2\pi} \int_{-\infty}^{\infty} r(k)e^{ik(x+y)} dk \\ + \int_x^\infty K_1(x, s)Ce^{-\kappa(s+y)} ds \\ + \int_x^\infty K_0(x, s) \left\{ \frac{1}{2\pi} \int_{-\infty}^{\infty} r(k)e^{ik(s+y)} dk \right\} ds = 0. \end{aligned} \quad (40)$$

The last term in the left-hand side of (40) can be simplified by changing the order of integration and inserting the explicit expression for $K_0(x, s)$ given in (39):

$$\begin{aligned} \int_x^\infty K_0(x, s) \left\{ \frac{1}{2\pi} \int_{-\infty}^{\infty} r(k)e^{ik(s+y)} dk \right\} ds \\ = \frac{1}{2\pi} \int_{-\infty}^{\infty} r(k)e^{iky} \left\{ \int_x^\infty -\frac{2\kappa Ce^{-\kappa(x+s)}}{2\kappa + Ce^{-2\kappa x}} e^{iks} ds \right\} dk \\ = K_0(x, x) \frac{1}{2\pi} \int_{-\infty}^{\infty} \frac{r(k)}{\kappa - ik} e^{ik(x+y)} dk. \end{aligned} \quad (41)$$

We now define an auxiliary function $f_1(x)$:

$$f_1(x) = \int_x^\infty K_1(x, s)e^{-\kappa s} ds, \quad (42)$$

and rewrite (40) to obtain

$$\begin{aligned} K_1(x, y) = -\frac{1}{2\pi} \int_{-\infty}^{\infty} r(k)e^{ik(x+y)} dk - Ce^{-\kappa y} f_1(x) \\ - K_0(x, x) \frac{1}{2\pi} \int_{-\infty}^{\infty} \frac{r(k)}{\kappa - ik} e^{ik(x+y)} dk. \end{aligned} \quad (43)$$

By substituting (43) into (42) we obtain

$$\begin{aligned} f_1(x) = - \int_x^\infty \left\{ \frac{1}{2\pi} \int_{-\infty}^{\infty} r(k)e^{ik(x+s)} dk \right\} e^{-\kappa s} ds \\ - f_1(x) \int_x^\infty Ce^{-2\kappa s} ds \\ - K_0(x, x) \int_x^\infty \left\{ \frac{1}{2\pi} \int_{-\infty}^{\infty} \frac{r(k)}{\kappa - ik} e^{ik(x+s)} dk \right\} \\ \times e^{-\kappa s} ds. \end{aligned} \quad (44)$$

Equation (44) is simplified by changing the order of integration and integrating with respect to the variable s . The result is

$$\begin{aligned} f_1(x) = -e^{-\kappa x} \frac{1}{2\pi} \int_{-\infty}^{\infty} \frac{r(k)}{\kappa - ik} e^{2ikx} dk - \frac{C}{2\kappa} e^{-2\kappa x} f_1(x) \\ - K_0(x, x) e^{-\kappa x} \frac{1}{2\pi} \int_{-\infty}^{\infty} \frac{r(k)}{(\kappa - ik)^2} e^{2ikx} dk. \end{aligned} \quad (45)$$

By solving (45) for $f_1(x)$ and substituting the result into (43) we obtain a solution to (19):

$$\begin{aligned}
 K_1(x, y) = & -\mathcal{F}_{x+y} [r(k)] \\
 & - K_0(x, x) \mathcal{F}_{x+y} \left[\frac{r(k)}{\kappa - ik} \right] \\
 & - K_0(x, y) \left(K_0(x, x) \mathcal{F}_{2x} \left[\frac{r(k)}{(\kappa - ik)^2} \right] \right. \\
 & \left. + \mathcal{F}_{2x} \left[\frac{r(k)}{\kappa - ik} \right] \right). \quad (46)
 \end{aligned}$$

The result gives an approximate solution to the GLM equation, $K(x, y) = K_0(x, y) + K_1(x, y)$, that is given in (23) in Section III.

REFERENCES

- [1] J. A. Dobrowolski and R. A. Kemp, "Refinement of optical multilayer systems with different optimization procedures," *Appl. Opt.*, vol. 29, pp. 2876–2893, 1990.
- [2] C. Styan, A. Vukovic, P. Sewell, and T. M. Benson, "An adaptive synthesis tool for rib waveguide design," *J. Lightw. Technol.*, vol. 22, no. 12, pp. 2793–2800, Dec. 2004.
- [3] E. Anemogiannis, E. N. Glytsis, and T. K. Gaylord, "Optimization of multilayer integrated optics waveguides," *J. Lightw. Technol.*, vol. 12, no. 3, pp. 512–517, Mar. 1994.
- [4] S. P. Yukon and B. Bendow, "Design of waveguide with prescribed propagation constants," *J. Opt. Soc. Amer.*, vol. 70, pp. 172–179, Feb. 1980.
- [5] A. K. Jordan and S. Lakshmanasamy, "Inverse scattering theory applied to the design of single-mode planar optical waveguides," *J. Opt. Soc. Amer. A*, vol. 6, pp. 1206–1212, Aug. 1989.
- [6] S. Lakshmanasamy and A. K. Jordan, "Design of wide-core planar waveguides by an inverse scattering method," *Opt. Lett.*, vol. 14, pp. 411–413, Apr. 1989.
- [7] L. S. Tamil and Y. Lin, "Synthesis and analysis of planar optical waveguides with prescribed TM modes," *J. Opt. Soc. Amer. A*, vol. 10, pp. 1953–1962, Sep. 1993.
- [8] D. B. Ge, A. K. Jordan, and L. S. Tamil, "Numerical inverse scattering theory for the design of planar optical waveguides," *J. Opt. Soc. Amer. A*, vol. 11, pp. 1863–1876, Nov. 1994.
- [9] C. Papachristos and P. Frangos, "Synthesis of single- and multi-mode planar optical waveguides by a direct numerical solution of the Gel'fand-Levitan-Marchenko integral equation," *Opt. Commun.*, vol. 203, pp. 27–37, 2002.
- [10] M. S. Sodha and A. K. Ghatak, *Inhomogeneous Optical Waveguides*. New York: Plenum, 1977, ch. 2.
- [11] M. J. Ablowitz and H. Segur, *Solitons and the Inverse Scattering Transform*. Philadelphia, PA: SIAM, 1981, ch. 1.
- [12] D. Marcuse, *Light Transmission Optics*. New York, Van Nostrand Reinhold: , 1982, ch. 1.
- [13] P. Yeh, *Optical Waves in Layered Media*. New York: Wiley-Interscience, 1988, ch. 5.
- [14] J. Xia, A. K. Jordan, and J. A. Kong, "Inverse-scattering view of modal structures in inhomogeneous optical waveguides," *J. Opt. Soc. Amer. A*, vol. 9, pp. 740–748, May 1992.
- [15] P. Deift and E. Trubowitz, "Inverse scattering on the line," *Commun. Pure Appl. Math.*, vol. 32, pp. 121–251, 1979.
- [16] D. G. Luenberger, *Linear and Nonlinear Programming*, 2nd ed. Boston, MA: Addison-Wesley, 1984, ch. 14.
- [17] G. H. Golub, P. C. Hansen, and D. P. O'Leary, "Tikhonov regularization and total least squares," *SIAM J. Matrix Anal. Appl.*, vol. 21, pp. 185–194, 1999.
- [18] E. Peral, J. Capmany, and J. Marti, "Iterative solution to the Gel'fand-Levitan-Marchenko coupled equations," *IEEE J. Quantum Electron.*, vol. 32, no. 12, pp. 2078–2084, Dec. 1996.
- [19] J. Skaar, L. Wang, and T. Erdogan, "On the synthesis of fiber Bragg gratings by layer peeling," *J. Lightw. Technol.*, vol. 37, no. 2, pp. 165–173, Feb. 2001.
- [20] A. Rosenthal and M. Horowitz, "Inverse scattering algorithm for reconstructing strongly reflecting fiber Bragg gratings," *IEEE J. Quantum Electron.*, vol. 39, no. 8, pp. 1018–1026, Aug. 2003.

Itay Hirsh was born in Kfar-Sava, Israel, in 1976. He received the B.Sc. degree in electrical engineering (with honors) in 2003 from the Technion - Israel Institute of Technology, Haifa, Israel, where he is currently working toward the M.Sc. degree in electrical engineering.

His research interests include inverse scattering theory in optical waveguides.

Moshe Horowitz received the Ph.D. degree from the Technion - Israel Institute of Technology, Haifa, Israel, in 1994.

Since 1997, he has been a faculty member in the Department of Electrical Engineering in the Technion. His current research interests include inverse scattering theory in fiber gratings, nonlinearity in Bragg gratings, novel fiber lasers, and microwave photonics.

Amir Rosenthal was born in Haifa, Israel, in 1981. He received the B.Sc. and Ph.D. degrees in 2002 and 2006, respectively, both from the Department of Electrical Engineering at the Technion - Israel Institute of Technology, Haifa, Israel.

He is currently a Postdoctoral Fellow at the Institute for Biological and Medical Imaging (IBMI), Technische Universitaet and Helmholtz Zentrum Muenchen, Germany. His research interests include optoacoustic imaging, inverse problems, and optical modeling.